

## Arsenate Zeolite Analogues with 11 Topological Types

Pingyun Feng,\* Tianzhi Zhang, and Xianhui Bu<sup>‡</sup>

Chemistry Department, University of California  
Riverside, California 92521

Received June 14, 2001

While there is always a general interest in discovering new open-framework materials in novel compositional domains,<sup>1–3</sup> our interest in arsenates also stems from our desire to understand roles of chemical and geometrical factors of precursor molecules in determining the composition and topology of the final product. When only the geometric factor is concerned, the arsenic system should be more like the germanate system because its ionic size ( $\text{As}^{5+}$ , 0.335 Å) is much closer to  $\text{Ge}^{4+}$  (0.39 Å) than to  $\text{P}^{5+}$  (0.17 Å).<sup>4</sup> On the other hand, when chemical factors such as atomic charge are concerned, the arsenate system would be expected to be more like the phosphate system. Thus, the study of the arsenate system affords a unique opportunity to investigate individual roles of chemical and geometric factors and their interplay in determining the final framework composition and topology.

An examination of known arsenates and phosphates with four-connected zeolite-type topologies shows two different aspects. In the  $\text{T}^{2+}/\text{T}^{5+}$  systems such as zincarsenates and zincophosphates (T refers to a tetrahedral atom) templated with alkali metal cations, both arsenate and phosphate structures can usually be made.<sup>5</sup> On the other hand, in the  $\text{T}^{3+}/\text{T}^{5+}$  system such as aluminarsenates and aluminophosphates, few tetrahedral arsenates with open framework topologies have been made even though many  $\text{AlPO}_4$  structures are known.<sup>6–10</sup> Thus, the first step in our overall synthetic strategy for developing tetrahedral arsenates is to combine the  $\text{T}^{2+}/\text{T}^{5+}$  and  $\text{T}^{3+}/\text{T}^{5+}$  systems and to synthesize ternary  $\text{T}^{2+}/\text{T}^{3+}/\text{T}^{5+}$  four-connected arsenates. Such a strategy also addresses a fundamental parameter in the formation of four-connected open frameworks: host–guest charge density matching. From earlier work on phosphates and germanates, we observed that regardless how well the geometrical conformation of a molecular template matches the internal pore geometry of a three-dimensional framework, the framework would not form unless the host–guest charge density also matches simultaneously.<sup>11–13</sup>

Both gallo- and aluminarsenates are investigated in this work, and zinc is selected as the divalent T-atom. A typical synthesis condition is as the following.<sup>14</sup>  $\text{As}_2\text{O}_5$  (0.711 g) and tris(2-aminoethyl)amine (1.470 g) were added to a mixed solvent containing  $\text{H}_2\text{O}$  (5.354 g) and ethyleneglycol (2.713 g). The mixture was stirred for 1 day before  $\text{Al}(\text{NO}_3)_3 \cdot 9\text{H}_2\text{O}$  (1.155 g) was added. After stirring for another day,  $\text{Zn}(\text{NO}_3)_2 \cdot 6\text{H}_2\text{O}$  (0.919 g), 49% HF (0.049

g), and pyridine (0.491 g) were added. The pH of the mixture was lowered to 5.23 with 2 M  $\text{HNO}_3$  (9.372 g). The mixture was heated in a Teflon-coated steel autoclave at 150 °C for 4 days, and clear crystals of zinc aluminarsenate with UCSB-7 topology were recovered. Other arsenate phases can be made by a similar procedure with different amines at different pH values.

From single-crystal structural analyses, 11 four-connected topologies (ABW, ANA, CHA, EDI, GIS, KFI, LAU, SOD, THO, UCSB-7, ACP-2) have been identified (Table 1).<sup>6,12,13</sup> Different chemical compositions with various lattice symmetries have also been made by changing types of  $\text{T}^{3+}$  atoms (Al or Ga),  $\text{T}^{3+}/\text{T}^{2+}$  ratios, and structure-directing agents. The coexistence of  $\text{T}^{2+}$  and  $\text{T}^{3+}$  cations can be inferred by the charge neutrality role when guest molecules are located. More generally, the average T–O bond distance can be used to estimate the  $\text{T}^{2+}/\text{T}^{3+}$  ratio by comparing the T–O distance to the pure  $\text{T}^{2+}$ –O and  $\text{T}^{3+}$ –O distance. For mixed  $\text{T}^{2+}/\text{T}^{3+}$  sites, the T–O distance would be intermediate between the pure  $\text{T}^{2+}$ –O and  $\text{T}^{3+}$ –O distances.<sup>12</sup>

To our knowledge,  $\text{AlAsO}_4$ –CHA is the first and only undoped aluminarsenate compound that has a structural analogue among aluminosilicate zeolites.<sup>6</sup> Because of the absence of divalent substitution, its framework is neutral like many  $\text{AlPO}_4$  phases. The protonated amine molecules (i.e., pyridine) are completely ordered, and their positive charges are balanced by hydroxyl groups that are attached to one-third of  $\text{Al}^{3+}$  sites, in a fashion similar to that found in some  $\text{AlPO}_4$ 's such as the ultra-large pore VPI-5.<sup>6</sup>

The size effect of the T-atom is shown in two different ways. One is in comparison with phosphates. Because of the larger size of  $\text{As}^{5+}$ ,  $\text{ZnAlAs}$ –THO (THO = Thomsonite) and  $\text{ZnAlAs}$ –2 are synthesized with 1,4-diaminobutane and 1,5-diaminopentane, whereas similar phosphate phases, ACP–THO (ACP = aluminum cobalt phosphate) and ACP-2 were made with 1,3-diaminopropane and 1,4-diaminobutane.<sup>12</sup> This is an interesting example that an increase in the T-atom size from  $\text{P}^{5+}$  to  $\text{As}^{5+}$  requires an extra methylene group in the structure-directing agent to have a better host–guest geometrical fit.  $\text{ZnAlAs}$ –2 has the same four-connected topology as that reported for ACP-2 and GCP-2, two cobalt phosphates substituted by  $\text{Al}^{3+}$  and  $\text{Ga}^{3+}$ , respectively.<sup>12</sup> Such a topology has not yet been found in either silicates or germanates.

A fundamentally different size effect is seen when a comparison is made with the germanate system. It is worth noting that the topology of UCSB-7 has not yet been found in either phosphates or silicates yet, but it frequently occurs in both germanate and arsenate systems.<sup>13</sup> Dozens of different amines can give rise to such a topology in either germanate or arsenate systems. This is apparently due to the similar ionic size between  $\text{Ge}^{4+}$  and  $\text{As}^{5+}$  cations. This is a very good example that shows that the stability of a given topology and the ease with which a given topology can be created are intimately related to the ionic size of the tetrahedral atom.

One benefit of working with the arsenate system over the germanate system is that the noncentrosymmetry of the UCSB-7 framework can be maintained when the framework negative charges are tuned by changing the  $\text{T}^{2+}/\text{T}^{3+}$  ratio. UCSB-7 has two helical 12-ring pore systems.<sup>13</sup> The two helical pore systems are left-handed and right-handed; however, they are not mirror images of each other when there are two unique, alternating T-atom sites. In the germanate system, when we attempt to enhance the framework stability by increasing the Ge/Ga ratio above 1 and decreasing the framework negative charge, the noncentrosymmetry is lost because of the disorder in T-atom sites.<sup>13</sup> On the other hand,  $\text{As}^{5+}$  sites and  $\text{T}^{2+}/\text{T}^{3+}$  sites are always alternating in arsenates, and the noncentrosymmetry is preserved at different framework charge density. This may have some implications as nonlinear optical materials or in their potential use as noncentric chiral hosts.

<sup>‡</sup> Santa Barbara, CA 93106.

(1) Wilson, S. T.; Lok, B. M.; Messina, C. A.; Cannan, T. R.; Flanigen, E. M. *J. Am. Chem. Soc.* **1982**, *104*, 1146–1147.

(2) Szostak, R. *Handbook of Molecular Sieves*; Van Nostrand Reinhold: New York, 1992.

(3) Ekambaram, S.; Sevov, S. C. *Inorg. Chem.* **2000**, *39*, 2405–2410.

(4) Shannon, R. D. *Acta Crystallogr.* **1976**, *A32*, 751–767.

(5) Gier, T. E.; Stucky, G. D. *Nature* **1991**, *349*, 508–510.

(6) Meier, W. M.; Olson, D. H.; Baerlocher, Ch. *Atlas of Zeolite Structure Types*; Elsevier: Amsterdam, 1996.

(7) Yang, G.; Li, L.; Chen, J.; Xu, R. *J. Chem. Soc., Chem. Commun.* **1989**, 810–811.

(8) Haushalter, R. C.; Wang, Z.; Meyer, L. M.; Dhingra, S. S.; Thompson, M. E.; Zubieta, J. *Chem. Mater.* **1994**, *6*, 1463–1464.

(9) Parish, J. B.; Corbin, D. R.; Gier, T. E.; Harlow, R. L.; Abrams, L.; von Dreele, R. B. *Zeolites* **1992**, *12*, 360–368.

(10) Wang, B.; Wang, S.; Lii, K. *Chem. Commun.* **1996**, 1061–1062.

(11) Bu, X.; Feng, P.; Stucky, G. D. *Science* **1997**, *278*, 2080–2085.

(12) Feng, P.; Bu, X.; Stucky, G. D. *Nature* **1997**, *388*, 735–741.

(13) Bu, X.; Feng, P.; Gier, T. E.; Zhao, D.; Stucky, G. D. *J. Am. Chem. Soc.* **1998**, *120*, 13389–13397.

(14) Arsenate compounds used in the synthesis may present a health or environmental hazard. Proper safety procedures and disposal rules should be followed in the handling of these compounds.

**Table 1.** Summary of Crystallographic Data for New Arsenate Phases Synthesized in This Study<sup>a</sup>

| name                    | formula   | amine <sup>b</sup>           | space group                         | <i>a</i> (Å) | <i>b</i> (Å) | <i>c</i> (Å) | $\beta$ (deg) | <i>R</i> ( <i>F</i> ) | $2\theta_{\max}$ | M–O (Å) |
|-------------------------|---|------------------------------|-------------------------------------|--------------|--------------|--------------|---------------|-----------------------|------------------|---------|
| ZnAsO <sub>4</sub> -ABW | NH <sub>4</sub> ZnAsO <sub>4</sub>  | NH <sub>4</sub> <sup>+</sup> | <i>P</i> 2 <sub>1</sub>             | 8.959        | 5.633        | 9.130        | 90.159        | 4.06                  | 56               | 1.950   |
| ZnAsO <sub>4</sub> -ANA | [Zn(H <sub>2</sub> O)]Zn <sub>3</sub> As <sub>3</sub> O <sub>12</sub>           | NH <sub>4</sub> <sup>+</sup> | <i>I</i> 2 <sub>1</sub> 3           | 13.853       | 13.853       | 13.853       | 90            | 6.19                  | 56               | 1.918   |
| ZnAsO <sub>4</sub> -CHA | (Zn)Zn <sub>6</sub> As <sub>6</sub> O <sub>24</sub>                             | R19                          | <i>R</i> -3                         | 13.838       | 13.838       | 15.971       | 90            | 6.13                  | 50               | 1.940   |
| AlAsO <sub>4</sub> -CHA | (Al <sub>3</sub> As <sub>3</sub> O <sub>12</sub> )(OH)                          | py                           | <i>P</i> -1                         | 9.422        | 9.476        | 9.643        | 86.582        | 3.47                  | 56               | 1.745   |
| ZnAsO <sub>4</sub> -EDI | (NH <sub>4</sub> ) <sub>3</sub> Zn <sub>5</sub> As <sub>5</sub> O <sub>20</sub> | R4                           | <i>P</i> -4                         | 10.192       | 10.192       | 27.550       | 90            | 4.15                  | 56               | 1.939   |
| ZnGaAs-GIS              | ZnGaAs <sub>2</sub> O <sub>8</sub>  | TMA                          | <i>C</i> 2/ <i>c</i>                | 15.424       | 9.796        | 10.874       | 134.29        | 3.36                  | 56               | 1.874   |
| ZnAlAs-GIS              | ZnAlAs <sub>2</sub> O <sub>8</sub>  | DMA                          | <i>C</i> 222 <sub>1</sub>           | 14.641       | 14.823       | 9.484        | 90            | 5.50                  | 56               | 1.833   |
| ZnAsO <sub>4</sub> -KFI | ZnZn <sub>6</sub> (AsO <sub>4</sub> ) <sub>6</sub>                              | R6                           | <i>P</i> <i>n</i> -3                | 18.965       | 18.965       | 18.965       | 90            | 4.97                  | 56               | 1.961   |
| ZnAlAs-LAU              | ZnAl <sub>2</sub> As <sub>3</sub> O <sub>12</sub>                               | py                           | <i>C</i> 2/ <i>c</i>                | 15.456       | 13.555       | 15.618       | 112.29        | 4.97                  | 56               | 1.809   |
| ZnGaAs-SOD1             | ZnGa <sub>2</sub> As <sub>3</sub> O <sub>12</sub>                               | TMA                          | <i>P</i> -43 <i>n</i>               | 9.1245       | 9.1245       | 9.1245       | 90            | 2.37                  | 56               | 1.872   |
| ZnAlAs-SOD              | ZnAl <sub>2</sub> As <sub>3</sub> O <sub>12</sub>                               | TMA                          | <i>P</i> -43 <i>n</i>               | 9.1343       | 9.1343       | 9.1343       | 90            | 1.38                  | 56               | 1.804   |
| ZnGaAs-SOD2             | Zn <sub>2</sub> GaAs <sub>3</sub> O <sub>12</sub>                               | pip                          | <i>P</i> -1                         | 9.4345       | 9.2805       | 8.5418       | 94.972        | 3.64                  | 56               | 1.905   |
| ZnAlAs-THO              | Zn <sub>4</sub> AlAs <sub>5</sub> O <sub>20</sub>                               | R4                           | <i>P</i> 2 <sub>1</sub> / <i>n</i>  | 13.453       | 14.666       | 14.666       | 90.197        | 14.4                  | 56               | 1.903   |
| ZnAlAs-2                | Zn <sub>3</sub> AlAs <sub>4</sub> O <sub>16</sub>                               | R5                           | <i>P</i> <i>b</i> <i>c</i> <i>m</i> | 9.0778       | 15.594       | 15.163       | 90            | 6.75                  | 56               | 1.876   |
| ZnGaAs-SV-1             | ZnGa <sub>2</sub> As <sub>3</sub> O <sub>12</sub>                               | TMA                          | <i>I</i> 4 <sub>1</sub> 32          | 18.623       | 18.623       | 18.623       | 90            | 2.38                  | 56               | 1.872   |
| ZnGaAs-SV-2             | Zn <sub>1-x</sub> Ga <sub>x</sub> AsO <sub>4</sub>                              | R3                           | <i>I</i> 4 <sub>1</sub> 32          | 18.600       | 18.600       | 18.600       | 90            | 3.69                  | 56               | 1.893   |
| ZnGaAs-SV-3             | Zn <sub>1-x</sub> Ga <sub>x</sub> AsO <sub>4</sub>                              | R4                           | <i>I</i> 4 <sub>1</sub> 32          | 18.705       | 18.705       | 18.705       | 90            | 4.47                  | 56               | 1.912   |
| ZnGaAs-SV-4             | Zn <sub>1-x</sub> Ga <sub>x</sub> AsO <sub>4</sub>                              | dabco                        | <i>I</i> 4 <sub>1</sub> 32          | 18.763       | 18.763       | 18.763       | 90            | 6.52                  | 50               | 1.898   |
| ZnAlAs-SV-1             | Zn <sub>2</sub> AlAs <sub>3</sub> O <sub>12</sub>                               | R14                          | <i>I</i> 4 <sub>1</sub> 32          | 18.624       | 18.624       | 18.624       | 90            | 4.54                  | 56               | 1.880   |
| ZnAlAs-SV-2             | Zn <sub>2</sub> AlAs <sub>3</sub> O <sub>12</sub>                               | R16                          | <i>I</i> 4 <sub>1</sub> 32          | 18.611       | 18.611       | 18.611       | 90            | 6.11                  | 50               | 1.876   |
| ZnAlAs-SV-3             | Zn <sub>2</sub> AlAs <sub>3</sub> O <sub>12</sub>                               | R20                          | <i>I</i> 4 <sub>1</sub> 32          | 18.568       | 18.568       | 18.568       | 90            | 4.71                  | 50               | 1.853   |
| ZnAlAs-SV-4             | Zn <sub>2</sub> AlAs <sub>3</sub> O <sub>12</sub>                               | lysine                       | <i>I</i> 4 <sub>1</sub> 32          | 18.561       | 18.561       | 18.561       | 90            | 4.45                  | 56               | 1.862   |

<sup>a</sup>  $R(F) = \sum |F_o| - |F_c| / \sum |F_o|$  with  $F_o > 4.0 \sigma(F)$ . Single-crystal data with Mo K $\alpha$ . In all formulas,  $x < 0.5$ . For ZnGaAs-SOD2,  $\alpha = 90.950(3)^\circ$ ,  $\beta = 94.972(2)^\circ$ ,  $\gamma = 90.149(3)^\circ$ , for AlAsO<sub>4</sub>-CHA,  $\alpha = 76.112(1)^\circ$ ,  $\beta = 86.582(1)^\circ$ ,  $\gamma = 89.094(1)^\circ$ . M–O is the average metal–oxygen bond distance. <sup>b</sup> TMA = (CH<sub>3</sub>)<sub>4</sub>N<sup>+</sup>; DMA = (CH<sub>3</sub>)<sub>2</sub>NH<sub>2</sub><sup>+</sup>; pip = piperazine; py = pyridine; dabco = 1,4-diazabicyclo[2.2.2]octane; R3 = NH<sub>2</sub>(CH<sub>2</sub>)<sub>3</sub>NH<sub>2</sub>; R4 = NH<sub>2</sub>(CH<sub>2</sub>)<sub>4</sub>NH<sub>2</sub>; R5 = NH<sub>2</sub>(CH<sub>2</sub>)<sub>5</sub>NH<sub>2</sub>; R6 = NH<sub>2</sub>(CH<sub>2</sub>)<sub>6</sub>NH<sub>2</sub>; R14 = NH<sub>2</sub>(CH<sub>2</sub>)<sub>3</sub>NH(CH<sub>2</sub>)<sub>2</sub>NH<sub>2</sub>; R16 = 2-(2-aminoethylamine)ethanol, H<sub>2</sub>NCH<sub>2</sub>CH<sub>2</sub>NHCH<sub>2</sub>CH<sub>2</sub>OH; R19 = 4-(aminomethyl)piperidine; R20 = *N*-(2-aminoethyl)pyrrolidine.

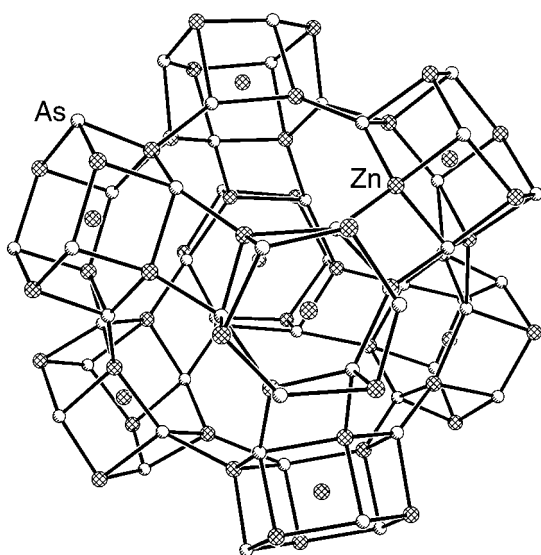


**Figure 1.**  $\alpha$ -Cage surrounded by eight double six-ring units in ZnAsO<sub>4</sub>-KFI. Framework oxygen atoms are omitted for clarity. Cross-hatched spheres represent Zn<sup>2+</sup> sites, whereas white spheres are As<sup>5+</sup> sites. Unconnected spheres are extra-framework Zn<sup>2+</sup> sites.

Three sodalite analogues reported here demonstrate that principles of host–guest charge-matching and symmetry-matching developed in the phosphate and germanate systems are equally applicable in the arsenate system.<sup>12,13</sup> While N(CH<sub>3</sub>)<sub>4</sub><sup>+</sup> cations with the three-fold symmetry give rise to a cubic sodalite lattice, protonated piperazine molecules bring the cubic symmetry of a regular sodalite lattice all the way down to the triclinic. Many dozens of sodalite analogues with various chemical compositions are known, but rarely has the sodalite lattice undergone such a dramatic reduction as that reported here.

The synthesis of gismondine analogues in both aluminato-, galloarsenate compositions (the structure type: GIS) and an aluminatoarsenate laumontite analogue (the structure type: LAU) illustrates that the arsenate system bears some similarities to silicates and phosphates. In particular, the gismondine topology constructed from the common 4.8.8 net is a frequent occurrence in the synthesis of either silicates or phosphates. The synthesis of the gismondine analogues suggests that other 4.8.8 net-based structure

types such as phillipsite and merlinoite might be accessible in the arsenate system.

Other topologies (ABW, analcime, chabazite, edingtonite, and ZK-5) have been made in the zinc arsenate system. Among these, the large cage ZK-5 analogue, ZnAsO<sub>4</sub>-KFI, is of particular interest because its structure is related to the commercially important zeolite A, but it has never been made before as a non-aluminosilicate despite extensive academic and industrial efforts in the exploration of phosphate-based molecular sieves.

With the exception of the ABW phase that is directed by ammonium cations only, the formation of analcime, chabazite, edingtonite, and ZK-5 phases requires the joint structure directing of two chemical species. For the edingtonite phase, both NH<sub>4</sub><sup>+</sup> cations and protonated 1,4-diaminobutane are included into the eight-ring channels. In the case of the chabazite and ZK-5 analogues, in addition to the protonated amine molecules, there is a Zn<sup>2+</sup> cation located at the center of each double six-ring secondary building unit (Figure 1). Similar charge-balancing Zn<sup>2+</sup> cations are also present in the analcime analogue.

In summary, it is shown that while the geometrical factor is the controlling factor in the synthesis of the four-connected UCSB-7 helical arsenate phases, the charge factor plays an important role in the synthesis of a number of structures that are analogues of phosphate phases. The interplay between the two factors allows the arsenate system to possess the structural characteristics of both phosphate and germanate systems. This explains why arsenates can adopt framework topologies that are unique either to the phosphate or germanate system. A peculiar feature of the arsenate system is the inclusion of divalent metals into structural subunits (e.g., double six-rings) of several analogues. With an enhanced understanding of various factors in the fabrication of zeolite-type frameworks, it is anticipated that more potentially useable microporous materials may be discovered by using the synthetic concept outlined here.

**Acknowledgment.** The financial support from UC Riverside to P. F. is gratefully acknowledged.

**Supporting Information Available:** Crystallographic data for all structures listed in Table 1 including positional parameters, thermal parameters, and bond distances and angles (PDF). This material is available free of charge via the Internet at <http://pubs.acs.org>.

JA0114658